Laboratory Investigation

Stress-Shortening Relations and Myocardial Blood Flow in Compensated and Failing Canine Hearts With Pressure-Overload Hypertrophy

William H. Gaasch, MD, Michael R. Zile, MD, Peter K. Hoshino, MD, Carl S. Apstein, MD, and Alvin S. Blaustein, MD

Serial changes in left ventricular (LV) size and function during the adaptation to chronic pressure overload and the transition to pump failure were studied in 16 conscious dogs (aortic bands placed at 8 weeks of age). Echocardiographic data at baseline and at 3, 6, 9, and 12 months after banding revealed a progressive increase in LV mass in all dogs. In six dogs with LV pump failure, there was a progressive decline in circumferential fiber shortening (29±4% at 12 months); this was significantly less than that seen in five littermate controls (38±3%, $p<0.05$). The average LV to body weight ratio in this group was 9.8±2.7 g/kg. In 10 dogs without pump failure (compensated LVH group), shortening exceeded that seen in the controls (43±4%, $p<0.05$); the LV to body weight ratio was 7.7±1.0 g/kg. At 12 months (cardiac catheterization), the LV end-diastolic pressure was higher in the failure (25±15 mm Hg) than in the compensated group (8±5 mm Hg, $p<0.05$); mean systolic stress was also higher in the failure group (313±67 g/cm^2) than in the compensated group (202±53 g/cm^2, $p<0.05$). The transmural distribution of myocardial blood flow was measured (at 12 months) with the radioactive microsphere technique; flow data were then related to an index of demand (a stress-time index). There was preferential blood flow to the subendocardial layers in the control (endo/epi=1.28) and compensated hearts (endo/epi=1.10), but in the failure group there was a relative decrease in subendocardial flow (endo/epi=0.92). However, the absolute values for subendocardial flow in the normal, compensated, and failure groups were 77±54, 125±48, and 113±64 ml/min/100 g; the stress-time indexes in the subendocardial shell were 38±11, 74±19, and 93±34 g sec · 10^2/cm^2/min. Despite what appears to be a marginal balance between blood flow and the stress time index in the failure group, the myocardial high energy phosphates were not depleted and the inoptropic state was not depressed. In this model of LV hypertrophy, the observed differences in fiber shortening can be explained on the basis of the inverse afterload-shortening relation; pump failure was due to an inadequate LV hypertrophy with afterload excess. Pump failure due to afterload excess was associated with adequate subendocardial blood flow at rest; during exercise or other hemodynamic stress, however, these hearts are likely to be especially vulnerable to ischemia and its consequences. (*Circulation* 1989;79:872–883)

The left ventricle adapts to a prolonged systolic pressure overload through a concentric hypertrophic process that results in an increased left ventricular (LV) wall thickness while maintaining a normal chamber volume. Thus, despite high intracavitary pressures, systolic wall stress (afterload) is not increased and fiber shortening (ejection fraction) is preserved. Eventually, afterload excess or depression of the myocardial inotropic state or both cause a decline in fiber shortening, and pump failure ensues. The time course of these changes and the mechanisms underlying this transition to failure are as yet not well understood.[1–8] Accordingly, a major goal of this research was to define the changes in LV size and function during the gradual development of concentric LV hypertrophy and to identify early mechanical markers of the transition to LV

From the Department of Medicine (Cardiology), The Medical Center of Central Massachusetts/Memorial, Worcester; the Cardiac Muscle Research Laboratory, Boston University School of Medicine, Boston; and the Veterans Administration Medical Center, Boston, Massachusetts.

Supported by medical research funds from the Veterans Administration, Washington, DC, and by Grant HL-31807 from the National Heart, Lung, and Blood Institute, Bethesda, Maryland.

Address for correspondence: William H. Gaasch, MD, Chief of Cardiology, The Medical Center/Memorial, 119 Belmont Street, Worcester, MA 01605.

Received June 20, 1988; revision accepted November 29, 1988.

pump failure; we also attempted to separate afterload excess from depressed inotropic state as a primary mechanism underlying pump failure.

A reduced coronary reserve that limits an adequate increase in myocardial blood flow during hemodynamic stress may be responsible for myocardial ischemia and depressed inotropic state that could contribute to pump failure in LV hypertrophy.[9-11] Intermittent ischemia might reduce glycogen or energy stores, limit or attenuate the hypertrophic response, and eventually lead to myocardial fibrosis—all of which could contribute chronically to LV pump failure. Under basal conditions, myocardial blood flow (flow per gram of tissue) is not depressed in most hypertrophied hearts, but the normal transmural perfusion gradient may decline during the stress of rapid pacing or exercise; the ratio of endocardial to epicardial flow falls below unity.[12,13] The failing hypertrophied heart may exhibit a similar relative subendocardial flow defect at rest despite an increase in absolute flow, which is presumably due to increased demands.[14] Therefore, a second objective of our research was to measure the transmural distribution of myocardial blood flow and to relate these data to derived indexes of demand (systolic stress and a stress-time index), to ventricular function, and to tissue high-energy phosphates. In this manner, we tested the hypothesis that a relative decrease in subendocardial blood flow is not necessarily associated with an imbalance between demand and flow, a depression of myocardial inotropic state, or a depletion of high energy phosphates.

Methods

A nonconstricting aortic band was applied to the ascending aorta of 8-week-old puppies, and serial studies of LV chamber size, myocardial mass, and ventricular function were performed during the following 12 months. During this period, there was a substantial increase in myocardial mass, and six of the 16 banded dogs developed evidence for LV pump failure. At 1 year, myocardial blood flow (MBF) was measured and the transmural distribution of blood flow was related to a systolic stress-time index and to measurements of tissue high-energy phosphates. All animals received humane care in compliance with the *Principles of Laboratory Animal Care* formulated by the National Society For Medical Research and the *Guide For the Care and Use of Laboratory Animals* prepared by the National Academy of Sciences and published by the National Institutes of Health (NIH Publication No. 85-23, revised 1985).

Surgical Procedure

The puppies were anesthetized with sodium pentobarbital (25 mg/kg, intravenously) and ventilated with a mechanical respirator. A right thoracotomy was performed through the third right intercostal space, the pericardium was opened, and the aorta was dissected free from the periaortic fat and connective tissue. A 5-mm wide polyethylene nonconstricting band was placed around the aorta approximately 2 cm above the aortic valve. In our initial studies, LV and aortic pressures were measured during application of the band. With slight traction on the band, we could produce a palpable thrill and 10–20 mm Hg pressure gradient across the area of the band; on release of traction, the pressure gradient was abolished. Based on this experience, we later discontinued pressure monitoring and simply placed the bands with no palpable thrill and no apparent constriction. After the banding procedure, the pericardium was loosely approximated, the thoracotomy was closed, and the pleural space was evacuated of air with a chest tube and suction. The animals recovered and serial echocardiographic studies were performed in the subsequent months. Five normal littermate puppies served as a control group.

Echocardiography

Each dog was lightly sedated with acepromazine (0.05–0.1 mg/kg i.v.) and suspended in a commercially available nylon sling (Chatham). Two-dimensional and M-mode echocardiographic LV studies (model SSH-10A, Toshiba, and model V-3280 B, Honeywell Electronics for Medicine) were obtained from the right parasternal area; the short-axis view including the minor axis dimension and wall thickness were readily visualized in all dogs, but the long axis of the LV chamber was not available in all dogs. These methods are similar to those reported by Morioka and Simon.[15] Echocardiographic studies were performed at 3-month intervals in all dogs and at 1- or 2-month intervals in most. At 6 and 12 months, the echocardiographic studies were performed during left heart catheterization (Figure 1).

Measurements of LV chamber dimension at end diastole (Ded) were made at the onset of the Q wave of the electrocardiogram; end-systolic dimension (Des) was measured at the time of the smallest (systolic) dimension, near the instant of maximum anterior motion of the LV posterior wall. The LV posterior wall thickness and the interventricular septal thickness were measured at end diastole by the leading edge technique, and myocardial cross-sectional area (CSA, cm^2) was calculated and used as an index of LV mass (see "Calculations" below). We have previously validated our echocardiographic CSA method over a wide range of LV mass in puppies and adults dogs with and without LV hypertrophy (LVH) ($n=44$); a highly significant correlation ($r=0.97$, $p<0.01$) between LV mass (weight at autopsy) and myocardial CSA (echocardiography) was found.[16]

Cardiac Catheterization

At 6 and 12 months after the banding procedure, the animals were lightly sedated with acepromazine and morphine sulfate; after using xylocaine anesthesia, an incision was made over a carotid artery. An

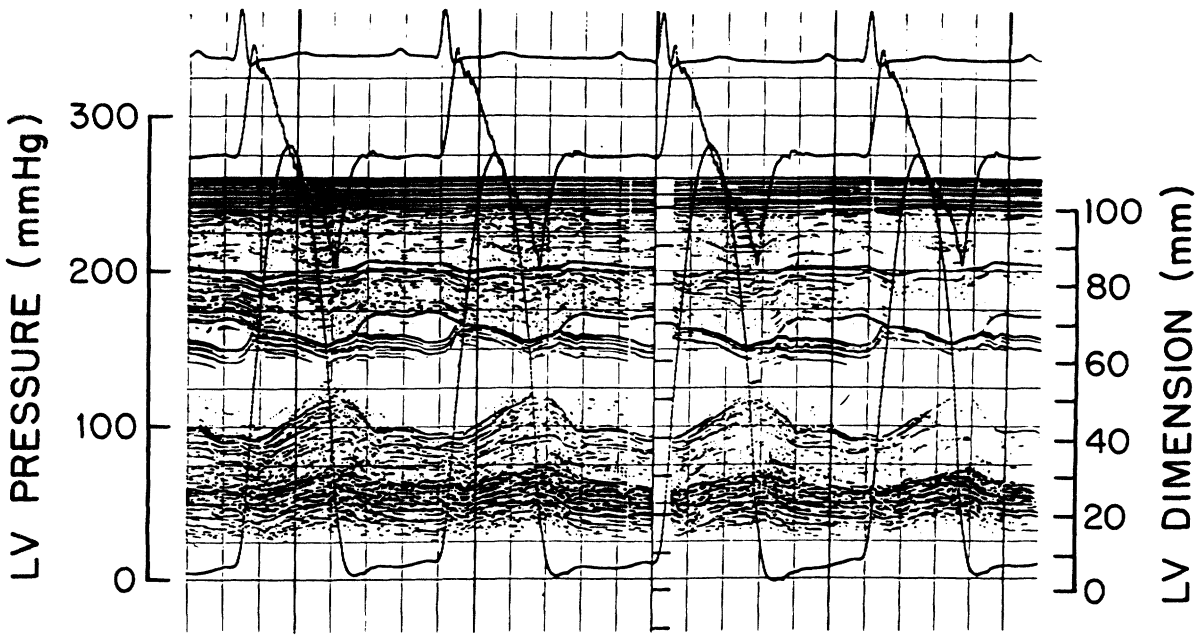

FIGURE 1. *Example of an echocardiographic-catheterization recording from a dog with compensated left ventricular hypertrophy (12 months). The left ventricular (LV) pressure is 275/12 mm Hg; the LV chamber size is normal (dimension, 32 mm), and the wall thickness is increased (12 mm). Endocardial shortening is supernormal (50%).*

arteriotomy was made and a 7F micromanometer-tipped catheter (Millar Instruments) was introduced and advanced into the left ventricle with fluoroscopic and hemodynamic guidance. A fluid-filled lumen in the catheter was connected to a transducer (P23dB, Statham) that was adjusted to midchest level; this second transducer was used to confirm the calibration of the micromanometer. Pressures in the aorta (above and below the band) and left ventricle and the time derivative of LV pressure were recorded with a photographic recorder (Honeywell, Electronics for Medicine). The catheter was secured and each dog was placed in the sling for simultaneous recording of the LV pressure and echocardiographic data. At the time of the 12-month study, the micromanometer was then replaced with LV and aortic catheters for determination of myocardial blood flow as described below. The catheters were removed, the arteriotomy was repaired or the artery was ligated, and the skin incision was closed.

Calculations

An index of LV mass was determined by calculating the myocardial cross-sectional area (CSA, cm^2) of the LV from the echocardiographic measurements:

$$CSA = \pi[(Ded/2) + Th]^2 - \pi(Ded/2)^2$$

where Ded is the LV chamber dimension at end diastole and Th is the LV wall thickness at end diastole (average of the septum and posterior wall). We and others have used this index of LV mass in clinical[17,18] and experimental[3] studies of LVH.

Circumferential fiber shortening at the endocardium (FSe, %), generally termed fractional shortening, was calculated with the standard method:

$$FSe = 100(Ded - Des)/Ded$$

where Ded is the chamber dimension at end diastole and Des is the dimension at end systole. In our laboratory, normal endocardial shortening exceeds 34%. Fiber shortening at the midwall was calculated with a model that does not require the conventional assumption that inner and outer wall thickening fractions are equal.[19] This model of nonuniform wall thickening provides shortening data that approximates the shortening of a theoretic circumferential midwall fiber; normal midwall shortening exceeds 19%.

Circumferential systolic wall stress was calculated as a function of radius from systolic pressure-geometry data (from the simultaneous catheter-echocardiography study) with a cylindric model.[20] Because of the substantial differences in LV wall thickness, the modified midwall method[19] was used to derive the midwall radius (r). Peak systolic stress (PSS, g/cm^2) at the midwall was calculated as:

$$PSS = P \times a^2[1 + (b^2/r^2)]/(b^2 - a^2)$$

where P is peak systolic pressure, a is the internal (endocardial) radius, b is the external (epicardial) radius, and r is the midwall radius. This index of peak systolic stress (calculated from dimensions at one third shortening) has been used in clinical[21] and experimental[22] studies of LV function and has been validated in patients with aortic valve disease.[23]

End systolic stress was calculated by substituting end systolic pressure-geometry data in the stress equation. Wall stress at the instant of aortic valve opening was also calculated by substituting the appropriate pressure-geometry measurements. Mean systolic wall stress during ejection was approximated by calculating the area under the three stress-time coordinates; this mean ejection stress (or shortening load) was used as the afterload parameter in the stress-shortening analysis. Thus, we assessed changes in mean circumferential shortening relative to mean circumferential stress during shortening.

An index of myocardial oxygen demand (a stress-time index) was calculated as the product of shortening load (the mean stress during shortening), the ejection period, and the heart rate (g sec · 10^2/cm^2/min). Shortening load was calculated at the middle of the inner half of the LV wall (inner shell) and at the middle of the outer half of the LV wall (outer shell); as before, stress was calculated as a function of radius.[18,19] Thus, a stress-time index for the inner and outer shells could be related to measurements of myocardial blood flow in the inner and outer shells.

Myocardial Blood Flow

Blood flow to the myocardium was determined by the radioactive microsphere technique.[24,25] Approximately 3 million spheres (3M Co), 15 μm in size, labeled with either ^{95}Nb, ^{141}Ce, ^{46}Sc, ^{103}Ru, or ^{113}Sn were injected into the left ventricle over a 15-second interval for each measurement. Beginning 5 seconds before injection, a reference sample of arterial blood was withdrawn from the aortic catheter at a constant rate of 15 ml/min for 90 seconds. The spheres were suspended in 10% dextran with 1 drop polysorbate 90 (TWEEN 80). The suspension was then vibrated for at least 1 hour in an ultrasonic cleaner; the dose to be injected was drawn into a 3-ml plastic syringe already containing 5 ml saline solution (constantly rotated to minimize settling or clumping) and administered within 3 minutes. The isotope was rotated for each experiment.

The heart was divided into four regions: the right and left atria, the right ventricular free wall, the interventricular septum, and the left ventricular free wall. The left ventricular free wall and interventricular septum was cut into rectangular blocks small enough to be sliced accurately into subendocardial and subepicardial halves. Reference blood samples and myocardial samples (3–4 g each) representing approximately two thirds of the total heart were counted for 10–20 minutes (minimum of 10,000 counts/sample) in a Packard series automatic gamma counting system, calibrated with ^{137}Cs.

Blood flow to each myocardial sample (Qm) was computed as:

$$Qm = Q_r \cdot C_m/C_r$$

where Q_r is reference blood flow (ml/min), C_m is counts/min of myocardial specimen, and C_r is counts/min of reference blood specimen. The blood flow from each myocardial section (ml/min) was divided by sample weight and expressed as milliliters per minute per gram of myocardium. Regional blood flow distribution was examined in four regions of the left ventricle: anterior and posterior portions of the interventricular septum as well as anterior and posterior portions of the LV free wall. Transmural blood flow distribution was also examined in the inner and outer half of the LV wall (subendocardial and subepicardial); this distribution was expressed in absolute numbers (ml/min/100 g) and also as a ratio of the subendocardial to subepicardial flow.

Biochemical Analysis

On the day after the 12-month catheterization study, the animals were anesthetized with sodium pentobarbitol (20 mg/kg) and ventilated with a mechanical respirator. A midline sternotomy was performed and the heart was placed on cardiopulmonary bypass. With a core biopsy tool connected to a suction device, a full-thickness sample of the LV free wall was taken and immediately frozen on dry ice. Each sample was divided equally into epicardial and endocardial halves, placed in liquid nitrogen, and stored for later determination of adenosine triphosphate (ATP) and creatine phosphate (CP); myocardial ATP and CP are expressed as micromoles per gram of dry tissue.[26,27]

Group Definitions and Data Analysis

Based on the 12-month hemodynamic (catheter-echocardiography) data, the 16 banded animals were divided into two groups. Assignment to the first group required a normal fractional shortening (greater than 34%); this group ($n=10$) was called LVH-compensated (LVH-C). A second group of six animals had reduced shortening; this group was called LVH-failure (LVH-F).

Data in the tables and text are presented as the mean ± SD; the mean ± SEM is used in the figures. The age and group effects were analyzed with a two-way analysis of variance; when appropriate, the Neuman-Keuls multiple sample comparison test was used to localize the significant differences. Differences in myocardial blood flow to the endocardial and epicardial shells were compared with a paired t test. Differences were considered statistically significant if the p value was less than 0.05.

Results

Serial measurements of end-diastolic dimension, myocardial cross-sectional area, fractional shortening, and animal weight are shown in Table 1; pressure, geometry, and mass data from the 12-month studies are shown in Table 2; myocardial blood flow, the stress-time index, and high-energy phosphate data are shown in Table 3.

Left Ventricular Size and Mass

The time course of change in LV minor axis dimension and myocardial cross-sectional area is

TABLE 1. Serial Changes in Left Ventricular Size and Function During the Development of Pressure-Overload Hypertrophy

	Baseline	3 Months	6 Months	9 Months	12 Months
Dimension at end diastole (mm)					
Control	23±3	35±5	36±4	38±5	39±4
LVH-compensated	23±2	29±3*	31±3*	33±2*	35±2*
LVH-failure	22±3	31±2	36±5†	40±2†	41±1†
Muscle cross-sectional area (cm^2)					
Control	6±1	9±3	10±2	11±3	12±2
LVH-compensated	5±1	9±2	12±4	16±3*	18±3*
LVH-failure	4±1	12±1*†	18±3*†	22±3*†	23±3*†
Endocardial shortening (%)					
Control	41±4	40±3	40±3	39±1	38±3
LVH-compensated	41±4	44±7	43±6	42±4	43±4*
LVH-failure	41±3	42±3	33±7†	32±7*†	29±4*†
Midwall shortening (%)					
Control	23±2	26±2	26±3	25±2	24±3
LVH-compensated	24±2	24±4	21±3*	20±3*	21±2*
LVH-failure	25±3	21±2*	17±3*†	18±3*	16±1*†
Body weight (kg)					
Control	6±1	17±5	22±6	23±6	23±4
LVH-compensated	6±1	15±5	19±6	20±6	20±6
LVH-failure	5±1	16±4	22±6	23±5	21±5

*$p<0.05$ vs. control.
†$p<0.05$ vs. LVH-C.

TABLE 2. Left Ventricular Pressure, Geometry, and Mass Data in Normal and Hypertrophied Hearts at 12 Months

	Control ($n=5$)	LVH-compensated ($n=10$)	LVH-failure ($n=6$)
Left ventricular pressure			
Peak systolic (mm Hg)	116±13	227±18*	259±74*
End diastolic (mm Hg)	7±3	8±5	25±15*†
Peak (+) dP/dt (mm Hg/sec)	3,032±530	3,057±964	2,925±954
Aortic pressure			
Systolic (mm Hg)	116±13	117±12	102±20
Diastolic (mm Hg)	79±19	82±13	75±23
Heart rate (beats/min)	82±25	124±35*	116±26*
Left ventricular echogram			
Dimension at end diastole (mm)	38.6±3.7	34.7±2.4*	41.0±0.9†
Dimension at end systole (mm)	24.0±2.9	19.6±2.4*	29.3±1.8*†
Endocardial shortening (%)	38±3	43±4*	29±4*†
Midwall shortening (%)	24±3	21±2*	16±1*†
Wall thickness (mm)	7.8±0.7	12.0±0.4*	13.0±0.6*
Myocardial cross-sectional area (cm^2)	11.8±2.0	17.7±2.8*	22.1±3.0*†
Left ventricular midwall stress			
Peak systolic (g/cm^2)	303±48	329±81	470±126*†
End systolic (g/cm^2)	141±35	82±35*	153±11†
Mean systolic (g/cm^2)	253±56	220±53	313±67†
Left ventricular mass			
LV weight (g)	98±27	144±33*	187±39*†
LV/body weight (g/kg)	4.4±0.8	7.7±1.0*	9.8±2.7*†

*$p<0.05$ vs. control.
†$p<0.05$ vs. LVH-comp.

TABLE 3. Myocardial Blood Flow, Stress-Time Index, and High-Energy Phosphate Data in Normal and Hypertrophied Hearts at 12 Months

	Control	LVH-compensated	LVH-failure
Myocardial blood flow (ml/min/100 g)			
Total left ventricle	69.0±47.9	119.9±51.0	124.0±37.4
Subendocardial shell	77.2±53.8	125.4±47.6	113.4±64.4
Subepicardial shell	61.8±44.8	118.2±54.2	133.0±96.3
Coronary blood flow (endo/epi ratio)	1.28±0.14	1.10±0.13*	0.92±0.1*†
Left ventricular mean systolic stress (g/cm^2)			
Subendocardial shell	296±59	281±65	379±81†
Subepicardial shell	230±53	187±46	271±58†
Left ventricular stress-time index (g sec·10^2/cm^2/min)			
Subendocardial shell	38±11	74±19*	93±34*
Subepicardial shell	30±9	50±13*	67±24*
Creatine phosphate (μm/g dry wt)			
Subendocardial	24.5±12.7	19.5±8.1	19.6±4.5
Subepicardial	20.2±9.3	19.1±4.8	21.5±4.4
Adenosine triphosphate (μm/g dry wt)			
Subendocarial	19.0±3.3	16.6±3.6	17.9±4.9
Subepicardial	17.1±2.1	17.8±2.7	18.7±3.3

*$p<0.05$ vs. control.
†$p<0.05$ vs. LVH-comp.

shown in Table 1 and Figure 2. As the animals grew, the end-diastolic dimension increased significantly during each of the first three intervals, there were no significant changes in dimension after the 9-month measurement (during the fourth interval). The end-diastolic dimension in the LVH-F group was not significantly different from the control group. There was a tendency for the dimension in the LVH-C group to be less than that seen in the other two groups; these differences were statistically significant at 3, 6, 9, and 12 months (all, $p<0.05$). However, when dimension was normalized for body weight, there were no differences among the three groups (Figure 2).

Myocardial cross-sectional area (CSA) increased significantly during the first two intervals in all three groups. Between 6 and 9 months, only the LVH groups demonstrated a continuing increase in CSA. After 9 months, there was no significant change in CSA. There was a significant difference in CSA between the control and LVH-C groups at 6, 9, and 12 months (all, $p<0.05$); CSA in the LVH-F group exceeded that seen in the other two groups at 3, 6, 9, and 12 months (all, $p<0.05$). When the CSA was normalized for body weight, the differences among the three groups persisted (Figure 2). Left ventricular weight (autopsy at 12 months), expressed as an absolute value (g) or normalized for body weight (g/kg), was substantially greater than normal in both groups with LVH; mass in the LVH-F group was greater than in the LVH-C group (Table 2).

In each of the three groups, there was a highly significant ($p<0.001$) increase in body weight during the first 6 months and there was no significant

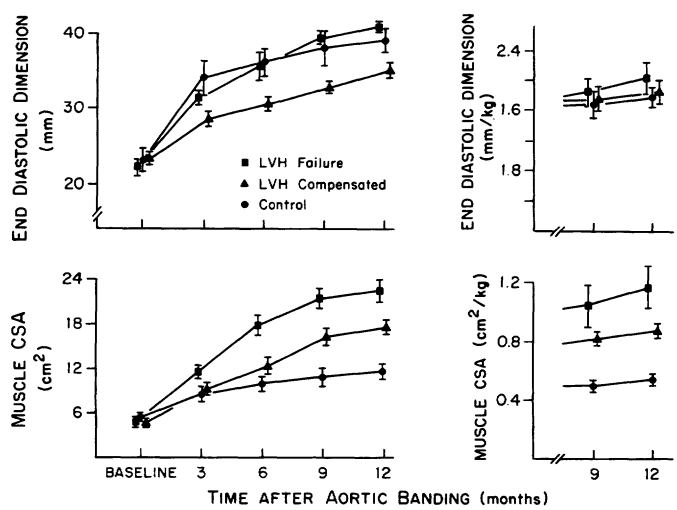

FIGURE 2. *Time course of change in left ventricular end-diastolic dimension and cross-sectional area (CSA) during the development of left ventricular hypertrophy (LVH). Most of the change in dimension and cross-sectional area occurred in the first 9 months. At 12 months, end-diastolic dimension in the compensated group was less than in the control and failure groups; however, when the dimension was normalized for body size there were no significant differences among the three groups. The LV CSA in the failure group was larger than that seen in the compensated group and both were greater than normal; when normalized for body size, these trends were still present.*

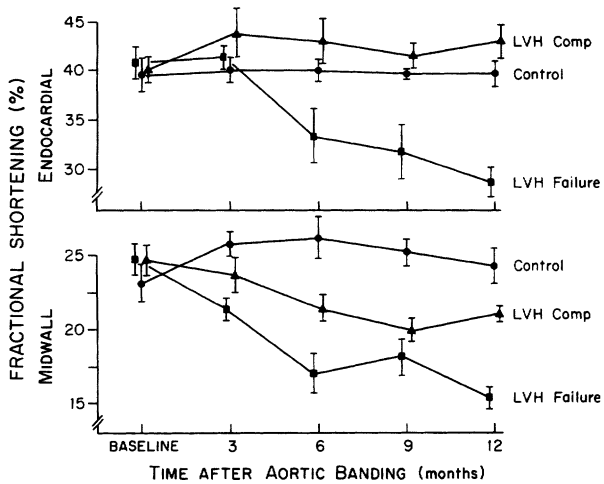

FIGURE 3. *The time course of change in left ventricular (LV) circumferential fiber shortening (fractional shortening) during the development of left ventricular hypertrophy (LVH). In compensated LVH, endocardial shortening exceeds normal while midwall shortening tends to be less than normal. In the LVH-failure group, midwall shortening became abnormal at 3 months and remained low thereafter, whereas endocardial shortening was significantly depressed at 6 months and thereafter. Thus, the earliest abnormality in fiber shortening was observed at the midwall of the failure group.*

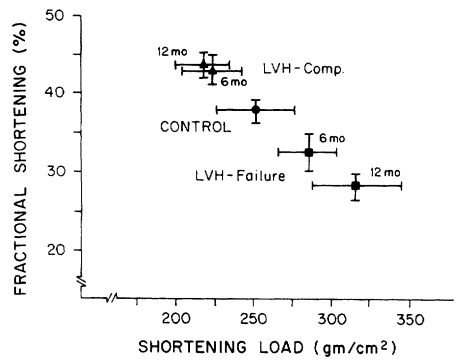

FIGURE 4. *Afterload-shortening relations in left ventricular hypertrophy (LVH). Circumferential fiber shortening is plotted against shortening load (mean stress during ejection). At 6 and 12 months, the compensated hearts (LVH-Comp, triangles) manifest increased shortening and a reduced load. The LVH-failure group (squares) exhibited a progressive increase in load and a decline in shortening. In this model of LVH, differences in shortening appear to be due to differences in shortening load (afterload mismatch).*

change in weight after 6 months. There were no significant differences among the three groups at baseline or at 3, 6, 9, and 12 months.

Left Ventricular Pressure

The LV pressure data are shown in Table 2. The average LV systolic pressure was highest in the LVH-F group, but the difference between the LVH-C and LVH-F groups did not achieve statistical significance. The average values for peak (+) dP/ dt were essentially equal in the three groups. The average LV end-diastolic pressure was normal in the LVH-C group (8±5 mm Hg) and elevated in the LVH-F group (25±15 mm Hg).

Fiber Shortening and Systolic Wall Stress

Serial changes in circumferential fiber shortening (both endocardial and midwall) are shown in Table 1 and Figure 3. At the time of the initial (baseline) study, there were no significant differences in endocardial or midwall shortening among the three groups. At 3 months and thereafter, there was a tendency for endocardial shortening in the LVH-C group to exceed that seen in the normal control group; this difference achieved statistical significance at 12 months. After 3 months, endocardial shortening in the LVH-F group progressively fell and was significantly less than normal at 6, 9, and 12 months.

In contrast to the endocardial measurements, midwall shortening in the LVH-C group declined and remained below that seen in the normal control group; while the difference in the average values (LVH-C compared with control) was statistically significant at 6, 9, and 12 months, six of the 10 LVH-C dogs remained within the range of normal (>19%). Midwall shortening in the LVH-F group was significantly less than that seen in the control group at 3 months, ($p<0.05$) and remained significantly below normal thereafter; at 12 months, midwall shortening was less than the lower limit of normal in all six dogs.

Peak systolic, end-systolic, and mean ejection stress (shortening load) at 12 months after banding are shown on Table 2. Peak and mean stresses in LVH-C were not significantly different from the average values for the normal control group; however, end-systolic stress was significantly less than normal. By contrast, the LVH-F group had significantly higher peak systolic stress compared with the control group; there was also a tendency for end-systolic stress and mean ejection stress to be higher than normal, but these differences did not achieve statistical significance. When the two LVH groups were compared, all three systolic stress parameters were significantly higher in the LVH-F group.

Afterload-shortening relations derived from the catheterization data are shown in Figure 4. This analysis demonstrates a distinct inverse relation between load and shortening; the LVH-C group exhibits increased shortening at low shortening load, whereas the LVH-F group exhibits reduced shortening at high shortening load.

Myocardial Blood Flow and the Stress-Time Index

These data are shown in Table 3 and Figure 5. When the transmural distribution of blood flow was examined, there was preferential flow to the suben-

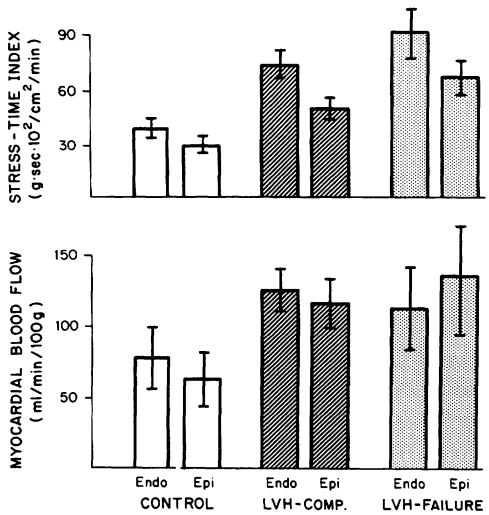

FIGURE 5. *Left ventricular (LV) stress-time index and myocardial blood flow in left ventricular hypertrophy (LVH). The stress-time index was higher in the subendocardial (endo) shell than in the subepicardial (epi) shell in all three groups. In the LVH-failure group, the subendocardial stress-time index was significantly greater than that seen in the control group; the myocardial blood flow appeared to be highest in the two LVH groups, but this trend did not achieve statistical significance.*

docardial layers in the normal control group (endo/epi=1.28); the subendocardial flow was significantly higher than the subepicardial flow ($p<0.05$). The differences were nonsignificant in the two LVH groups. The endo/epi flow ratio was 1.10 in the LVH-Comp group and 0.92 in the LVH-F group. Despite this relative decrease in subendocardial flow, the absolute value for myocardial blood flow in the subendocardial shell was not less than normal; indeed, there was a tendency for the absolute values to be somewhat higher than that seen in the normal control hearts. The average values for myocardial blood flow (ml/min/100 g myocardium) in the two groups with LVH exceeded that found in the normal control animals, but these differences did not reach statistical significance; likewise, there was no significant difference in the average values between the two groups with hypertrophy.

All three groups exhibited a transmural stress gradient with the highest values in the subendocardial shell. The stress-time index in the subendocardial shell was significantly higher than normal in the LVH-C group and the LVH-F group; the difference between the two groups with LVH did not achieve statistical significance. Likewise, there was a tendency for myocardial blood flow to be highest in the hypertrophied hearts (Table 3). The average values for the ratio of stress-time to myocardial blood flow (in the subendocardial shell) were 0.78 ± 0.26 in the normal control group, 0.67 ± 0.38 in the LVH-C group, and 0.97 ± 0.42 in the LVH-F group; there were no significant differences among the three groups. These data indicate that there was no imbalance between demands and blood flow in the LVH-F group.

Tissue High-Energy Phosphates

These data are shown in Table 3. There were no significant differences in CP or ATP among the three groups. Thus, in the presence of LV afterload excess, reduced fractional shortening, elevated end diastolic pressure, and marginal subendocardial perfusion, the LVH-F group did not exhibit depletion of myocardial high energy phosphates.

Discussion

The progression of pressure-overload LV hypertrophy from an initial phase of physiologic adaptation to the development of heart failure is a complex pathophysiologic process that is incompletely understood. Several experimental studies have been directed toward this area, but broad conclusions have been limited by difficulties with interrelating the results of different protocols in which a limited number of parameters was assessed. For example, Bache and associates have reported detailed measurements of myocardial perfusion in pressure-overload hypertrophy, but concomitant measures of wall stress and fiber shortening were not made.[12–14] Similarly, Wisenbaugh and associates assessed changes in myosin ATPase activity in hypertrophied hearts, but the adequacy of myocardial perfusion in their model was not reported.[6] Others have measured mechanical parameters but not myocardial perfusion or biochemistry.[3] It is also difficult to assess whether different investigators have used hypertrophied hearts at a comparable phase in the progression from adaptation to failure. As hypertrophy develops, the transition from a state of adaptation to failure undoubtedly depends on the relation between myocyte growth and capillary growth, the adequacy of myocardial perfusion and energy metabolism, and the mechanical workload. Therefore, we designed the current study to measure LV size and function serially after aortic banding. Then, myocardial mechanics, perfusion, and metabolism were assessed and analyzed according to the presence or absence of LV "pump failure."

We report six principal findings of our experiments. 1) Twelve months after aortic banding, LV afterload excess was present in six of the 16 dogs; the LV end-diastolic pressure was elevated but there was no chamber dilatation. 2) As early as 3 months after banding, the six dogs that would eventually develop LV pump failure exhibited a larger LV mass and a lower midwall shortening than the group that remained compensated; abnormalities of midwall shortening were observed before endocardial shortening was significantly depressed. 3) The LVH-F group appeared to fall on the same load-shortening relation as the control and LVH-C groups suggesting that the pump failure in the LVH-F group was due to afterload excess, not a depression of inotropic state. 4) There was a relative redistribution

of myocardial blood flow away from the endocardium in the LVH-F group, but the absolute values for subendocardial flow were not reduced. 5) The stress-time index was highest in the LVH-F group, but the ratio of stress-time to myocardial blood flow was not significantly different among the three groups. 6) Despite the presence of pump failure and marginal subendocardial blood flow, myocardial high energy phosphates were not depressed.

Model of Pressure-Overload Hypertrophy

When an aortic band is placed in young animals and concentric hypertrophy develops gradually, it is possible to obtain a substantial increase in LV mass; this, of course, depends on several factors, including the size of the band and the duration of the experimental protocol. One year after banding, our animals exhibited a 40–100% increase in the ratio of LV weight to body weight. Thus, the degree of LV hypertrophy in our animals is similar to that reported by others.[3,10,14,28] Hypertrophy in this model represents the additive effects of physiologic hypertrophy (normal growth) and pathologic hypertrophy (pressure overload). For this reason the results may not be equivalent to those that occur when a similar stimulus (systemic hypertension) occurs in an adult or aged animal. We find this canine model especially valuable because it can be studied with the same catheter-echocardiography methods that we use in humans.

Definition of Functional Compensation and Pump Failure

Pressure overload of the LV results in a series of compensatory morphologic, functional, and metabolic adjustments that make it difficult to develop a precise and uniformly applicable definition of LV failure in hypertrophic hearts.[8,29] Therefore, we used a standard clinical definition to separate our hypertrophied hearts into compensated and failure categories; hearts with normal endocardial fiber shortening (analogous to a normal ejection fraction) were placed in the compensated category while those with depressed shortening were placed in the pump failure group. All ten in the compensated (LVH-C) group had normal or near-normal LV end-diastolic pressure (<19 mm Hg), while five of the six in the failure (LVH-F) group had an elevated end-diastolic pressure (>19 mm Hg). In a similar fashion, Parrish et al[14] used end-diastolic pressure and Wisenbaugh et al[6] used shortening measurements to describe LV performance in dogs and pigs with pressure-overload hypertrophy. Data from these and other clinical and experimental studies of pressure overload hypertrophy are consonant with the definition of pump failure used in our current studies; this term does not indicate nor should it imply whether the pump failure is due to afterload excess, depression of the inotropic state, or a combination of the two.

Serial Changes in Left Ventricular Mass and Function

A major purpose of this study was to define the time course of change in LV mass and function during the development of pressure-overload hypertrophy and, in particular, to identify the earliest functional changes in the group that would eventually manifest pump failure. The serial echocardiographic data (Figure 2) illustrate a progressive increase in LV chamber dimension throughout the entire 12-month period of study, but most of this change occurred during the early months of the study when the animals were growing rapidly. In the group with compensated hypertrophy (LVH-C), the absolute measurements of chamber dimension were less than that seen in the other two groups, but when normalized for body size, there were no significant differences in chamber size among the three groups. Thus, there was no evidence for chamber dilatation in the group with failure (LVH-F).

The major increment in myocardial mass occurred within the first 6 months of study; between 6 and 9 months, the muscle CSA had reached a plateau in all three groups. In the dogs with LVH, myocardial mass (CSA by echocardiography and weight at autopsy) was substantially greater than normal at 1 year—even after normalization for body size; the highest values were found in the LVH-F group. This association between extreme LVH and LV pump dysfunction has been observed in clinical[8] and experimental studies,[6,14] and it may be that the development of massive hypertrophy and eventually a stage of exhaustion and myocardial failure occurs in the hearts with the greatest hemodynamic burden (i.e., the highest values for systolic wall stress). As will be discussed below, the reduced shortening in our LVH-F group was due to afterload excess; we did not demonstrate a significant imbalance between the stress-time index and myocardial blood flow, nor was there a depletion of high-energy phosphates. We, therefore, conclude that these hearts had not yet entered a state of exhaustion.

Measurements of endocardial and midwall shortening revealed significant differences amongst the three groups as early as 3–6 months after banding (Figure 3). Those in the LVH-C group exhibited a tendency toward increased endocardial shortening; this is analogous to the increased ejection fraction that is seen in patients with congenital valvular aortic stenosis.[30,31] Based on an analysis of LV wall stress-shortening data from patients with valvular aortic stenosis[30,31] and animals with aortic bands,[32,33] it appears that geometric changes in association with relatively low late systolic wall stress can account for this pattern of increased endocardial shortening in the presence of normal (or even marginally subnormal) shortening of the midwall fibers. Seven of the 10 animals in this LVH-C group exhibited midwall shortening values that were well

within the range of normal (>19%). By contrast, the group that eventually developed pump failure showed a progressive decline in midwall shortening that achieved statistical significance at three months and remained abnormal thereafter; at 12 months, the midwall shortening was abnormal in all six dogs. Values for endocardial shortening were not significantly lower than baseline until 6 months. Thus, the earliest detectable shortening abnormality in the LVH-F group was seen at the midwall.

Dumesnil and associates have indicated that endocardial shortening (and ejection fraction) is dependent not only on the average midwall fiber shortening but also on the geometry of the left ventricle; for a given extent of midwall shortening, the ejection fraction (endocardial shortening) will vary with the ratio of radius to thickness (or volume to mass) and, thus, systolic wall thickening in hypertrophic hearts contributes to ejection more than systolic thickening in normal hearts.[34,35] Because we set out to assess shortening differences in hearts with widely differing geometry, we measured both endocardial and midwall length transients. We do, however, place a special significance on the midwall shortening in part because the fibers at the midwall are anatomically oriented in a circumferential direction and especially because our calculated values for midwall stress are oriented in the same direction as the fibers.

A conventional stress-shortening analysis, shown in Figure 4, indicates that the differences in shortening between the LVH-C and LVH-F groups are primarily, if not entirely, due to differences in afterload. The unloading and increased shortening seen in our LVH-C group is similar to that described by Sasayama et al[32] in their experimental studies of hypertrophy with "hyperfunction and normal inotropic state." By contrast, the LVH-F group exhibited increased load and depressed shortening. The average value for fractional shortening at 12 months was 29%; while significantly less than the average value for the normal group, this does not represent a substantial decline in shortening (as might occur with combined afterload excess and depressed inotropic state). Furthermore, the values for peak (+) dP/dt were essentially equal in the three groups; this also supports our impression that changes in inotropic state do not contribute in a major way to the observed differences in shortening.

Myocardial Blood Flow

The ascending aortic constriction model differs from the valvular stenosis model of LVH in that systolic pressure below the aortic band (and in the proximal coronary arteries) can be substantially higher in the former than in the latter. There is, however, no diastolic pressure gradient across the aortic band and, thus, diastolic perfusion pressure in the proximal coronary arteries is well within the range of normal (similar to or slightly higher than may be seen in valvular stenosis). Therefore, even though proximal or epicardial coronary pressure and flow during systole may differ in valvular and supravalvular stenosis, it appears that diastolic flow and transmural perfusion are similar in these two models and in LVH due to hypertension.[36] Because myocardial blood flow occurs principally in diastole and the diastolic perfusion pressure was essentially normal in all three groups, the observed changes in the distribution of blood flow are not likely due to alterations in perfusion pressure that are peculiar to the aortic band model of pressure-overload hypertrophy.

Based on studies that indicate an elevated "minimal coronary vascular resistance" in LVH, it has generally been concluded that systolic pressure overload causes an increase in LV mass that is not matched by an appropriate functional growth of the coronary vasculature.[36] Thus, myocardial blood flow under basal conditions may be adequate, but the stress of exercise or pacing tachycardia may produce an imbalance between flow and demand[12,13]; experimental and clinical experience indicates that this functional deficit can result in myocardial ischemia or angina pectoris—even in patients with angiographically normal coronoary arteries. Thus, a loss of coronary vascular reserve might be responsible for myocardial ischemia and consequently to the development of LV failure. Until recently, however, there have been no published data on myocardial perfusion in hypertropic failing hearts.

As part of a series of seminal articles on myocardial perfusion in LV hypertrophy, Bache and associates[14] have shown that failing hearts exhibit changes in myocardial blood flow that are similar to those seen during pacing or exercise stress in compensated hypertrophy. In four dogs with substantial hypertrophy and failure (elevated LV end-diastolic pressure), they found that the absolute values for myocardial blood flow were increased, presumably due to an increased myocardial oxygen demand associated with elevated systolic wall stress; despite a high total flow, the ratio of subendocardial to subepicardial flow (endo/epi) in the failing hearts was significantly less than normal. We, too, found a highly significant transmural redistribution of myocardial blood flow in the LVH-F group (endo/epi=0.92), but the ratio of demand to flow (i.e., stress-time/flow) was not significantly higher than normal. This would be expected to produce ischemia during exercise or other hemodynamic stress, unless there is increased arteriovenous oxygen extraction or increased efficiency of the subendocardial myocardium. Unfortunately, it was not possible to make measurements of subendocardial oxygen consumption or lactate extraction (or production). We did, however, measure myocardial high-energy phosphates, and despite what appears to be marginal perfusion of the subendocardial shell of myocardium, we did not find a significant reduction in high-energy phosphates in the LVH-F group. These data can be taken as indirect evidence against persistent subendocardial ischemia in the LVH-F group.

The literature on myocardial high-energy phosphate concentration in hypertrophy includes data from failing and nonfailing hearts as well as experiments in which the adequacy of myocardial perfusion was not established.[37] Thus, some investigators have found reduced ATP content in hearts with pressure-overload hypertrophy[38] and some have not.[39] A relative ischemia as a consequence of experimental conditions likely caused a decline in high-energy phosphates in some studies, but in our experiments, the absolute values for subendocardial blood flow and the ratio of stress-time to blood flow were not significantly different from normal, and the high-energy phosphate content was normal.

In a large animal study of pressure-overload hypertrophy, Wisenbaugh et al[6] found that the myocardial ATPase activity was normal regardless of the degree of hypertrophy. Our animals had a similar degree of hypertrophy, a similar spectrum of normal and abnormal LV pump function, and normal myocardial ATP. Thus, the results of these two studies are quite complementary. When these data are viewed in conjunction with our myocardial blood flow data and those of Bache et al[12–14] and others,[10,11] it appears that pressure overload hypertrophy may progress to a stage of pump failure (afterload excess and elevated end-diastolic pressure) with marginal myocardial blood flow but no depression of myosin ATPase activity or depletion of high-energy phosphates. Hypertrophic hearts with pump failure exhibit afterload excess because LV wall thickness does not increase in proportion to the product of systolic pressure and radius. This could occur, in part, as a consequence of impaired myocardial protein synthesis due to intermittent myocardial ischemia. Such a speculation is based on the observation that myocardial protein synthesis, an energy-dependent process, is inhibited by hypoxia or ischemia.[40] Further research will be necessary if we are to understand better the transition to failure, but it is likely that increased afterload contributes to an increased oxygen demand such that a vicious cycle develops with worsening tissue ischemia and progression to a state of myocardial exhaustion and failure.

References

1. Linzbach AJ: Heart failure from the point of view of quantitative anatomy. *Am J Cardiol* 1960;5:370–382
2. Meerson FZ: The myocardium in hyperfunction, hypertrophy, and heart failure. *Circ Res* 1969;25(suppl II):II-1–II-163
3. Sasayama S, Ross J Jr, Franklin D, Bloor CM, Bishop S, Dilley RB: Adaptations of the left ventricle to chronic pressure overload. *Circ Res* 1975;38:172–178
4. Grossman W: Cardiac hypertrophy: Useful adaptation or pathologic process? *Am J Med* 1980;69:576–584
5. Krayenbuehl HP, Hess O, Herzel H: Pathophysiology of the hypertrophied heart in man. *Eur Heart J* 1982; 3(suppl A):125–131
6. Wisenbaugh T, Allen P, Cooper G IV, Holzgrefe H, Beller G, Carabello B: Contractile function, myosin ATPase activity and isozymes in the hypertrophied pig left ventricle after a chronic progressive pressure overload. *Circ Res* 1983; 53:332–341
7. Panidis IP, Kotler MN, Ren J, Mintz GS, Ross J, Kalman P: Development and regression of left ventricular hypertrophy. *J Am Coll Cardiol* 1984;3:1309–1320
8. Hamrell BB, Alpert NR: Experimental myocardial hypertrophy, in Levine HJ, Gaasch WH (eds): *The Ventricle: Basic and Clinical Aspects*. Boston, Martinus-Nijhoff, 1985, pp 185–207
9. Hoffman JIE: Determinants and prediction of transmural myocardial perfusion. *Circulation* 1978;58:381–391
10. Rembert JC, Kleinman LH, Fedor JM, Wechsler AS, Greenfield JC Jr: Myocardial blood flow distribution in concentric left ventricular hypertrophy. *J Clin Invest* 1978;62:379–386
11. Marcus ML, Doty DB, Hiratzka LF, Wright CB, Eastham CL: Decreased coronary reserve—A mechanism for angina pectoris in patients with aortic stenosis and normal coronary arteries. *N Engl J Med* 1982;307:1362–1367
12. Bache RJ, Vrobel TR, Ring WS, Emery RW, Anderson RW: Regional myocardial blood flow during exercise in dogs with chronic left ventricular hypertrophy. *Circ Res* 1981;48:76–87
13. Bache RJ, Vrobel TR, Arentzen CE, Ring WS: Effect of maximal coronary vasodilation on transmural myocardial perfusion during tachycardia in dogs with left ventricular hypertrophy. *Circ Res* 1981;49:742–750
14. Parrish DG, Ring WS, Bache RJ: Myocardial perfusion in compensated and failing hypertrophied left ventricle. *Am J Physiol* 1985;249:H534–H539
15. Morioka S, Simon G: Echocardiographic evidence for early left ventricular hypertrophy in dogs with renal hypertension. *Am J Cardiol* 1982;49:1890–1895
16. Izzi G, Hoshino PK, Zile MR, Gaasch WH: Validation of echocardiographically derived muscle cross sectional area as an index of left ventricular mass in dogs with and without pressure overload hypertrophy. *Clin Res* 1986;34:858A
17. Gaasch WH, Andrias CW, Levine HJ: Chronic aortic regurgitation: The effect of aortic valve replacement on left ventricular volume, mass and function. *Circulation* 1978; 58:825–836
18. Carroll JD, Gaasch WH, Zile MR, Levine HJ: Serial changes in left ventricular function after correction of chronic aortic regurgitation: Dependence on early changes in preload and subsequent regression of hypertrophy. *Am J Cardiol* 1983; 51:476–482
19. Shimizu G, Zile MR, Blaustein AS, Gaasch WH: Left ventricular chamber filling and midwall fiber lengthening in patients with left ventricular hypertrophy: Overestimation of fiber velocities by conventional midwall measurements. *Circulation* 1985;71:266–272
20. Timoshenko S, Goodier JN: *Theory of Elasticity*. New York, McGraw-Hill, 1951, pp 55–130
21. Gaasch WH, Battle WE, Oboler AA, Banas JS, Levine HJ: Left ventricular stress and compliance in man with special reference to normalized ventricular function curves. *Circulation* 1972;45:746–762
22. Mirsky I, Pfeffer JM, Pfeffer MA, Braunwald E: The contractile state as the major determinant in the evolution of left ventricular dysfunction in the spontaneously hypertensive rat. *Circ Res* 1983;53:767–778
23. Schwartz F, Flameng W, Langebartels F, Sesto M, Walter P, Schlepper M: Impaired left ventricular function in chronic aortic valve disease: Survival and function after replacement by Bjork-Shiley prosthesis. *Circulation* 1979;60:48–58
24. Neill WA, Phelps NC, Oxendine JM, Mahler DJ, Sim DM: Effect of heart rate on coronary blood flow distribution in dogs. *Am J Cardiol* 1973;32:306–312
25. Zile MR, Neill WA, Gaasch WH, Oxendine J, Apstein CS, Weinberg E, Bing OHL: Distribution of a neutral cardioplegic vehicle during the development of ischemic myocardial contracture. *J Mol Cell Cardiol* 1987;19:977–989
26. Bucher T: Uber ein phosphatubertragendes Garungsferment. *Biochem Biophys Acta* 1947;1:292–314
27. Adams H: Adenosine 5′triphosphate determination with phosphoglycerate kinase, in Bergmeyer HV (ed): *Methods of Enzymatic Analysis*. New York, Academic Press, 1963, pp 539–543

28. Fujii AM, Vatner SF, Serur J, Als A, Mirsky I: Mechanical and inotropic reserve in conscious dogs with left ventricular hypertrophy. *Am J Physiol* 1986;251:H815–H823
29. Ross J Jr: Afterload mismatch and preload reserve: A conceptual framework for the analysis of ventricular function. *Prog Cardiovasc Dis* 1976;18:255–264
30. Donner R, Carabello BA, Black I, Spann JF: Left ventricular wall stress in compensated aortic stenosis in children. *Am J Cardiol* 1983;51:946–951
31. Borow KM, Colan SD, Neuman A: Altered left ventricular mechanics in patients with valvular aortic stenosis and coarctation of the aorta: Effects on systolic performance and late outcome. *Circulation* 1985;72:515–522
32. Sasayama S, Franklin D, Ross J Jr: Hyperfunction with normal inotropic state of the hypertrophied left ventricle. *Am J Physiol* 1977;232:H418–H425
33. Hoshino PK, Zile MR, Blaustein AS, Gaasch WH: Systolic hyperfunction in pressure overload left ventricular hypertrophy. *Circulation* 1986;74(suppl II):397A
34. Dumesnil JG, Shoucri RM, Laurenceau JL, Turcot J: A mathematical model of the dynamic geometry of the intact left ventricle and its application to clinical data. *Circulation* 1979;59:1024–1034
35. Dumesnil JG, Shoucri RM: Effect of the geometry of the left ventricle on the calculation of ejection fraction. *Circulation* 1982;65:91–98
36. Alyono D, Anderson RW, Parrish DG, Dai XZ, Bache RJ: Alterations of myocardial blood flow associated with experimental canine left ventricular hypertrophy secondary to valvular aortic stenosis. *Circ Res* 1986;58:47–57
37. Fanburg BL: Experimental cardiac hypertrophy. *N Engl J Med* 1970;282:723–732
38. Peyton RB, Jones RN, Attarian D, Sink JD, Van Tright P, Currie WD, Wechsler AS: Depressed high-energy phosphate content in hypertrophied ventricles of animals and man: The biologic basis for increased sensitivity to ischemic injury. *Ann Surg* 1982;196:278–284
39. Wexler LF, Lorell BH, Momomura S, Weinberg ED, Ingwall JS, Apstein CS: Enhanced sensitivity to hypoxia-induced diastolic dysfunction in pressure-overload hypertrophy in the rat: Role of high energy phosphate depletion. *Circ Res* 1988;62:766–775
40. Morgan HE, Chua BHL, Watson PA, Russo L: Protein synthesis and degradation, in Fozzard HA, et al (eds): *The Heart and Cardiovascular System.* New York, Raven Press, 1986, chap 45

KEY WORDS • heart failure • myocardial blood flow • stress-time index • ventricular function • hypertrophy